THE EFFECT OF PROCESSING PARAMETERS ON SOL GEL SYNTHESIS OF β-SiC NANO POWDER

A. Najafi[1,*], F. Golestani-Fard[2,3] and H. R. Rezaie[2,3]

* *ab_najafi@iust.ac.ir*

Received: July 2013 **Accepted: January2014**

[1] Department of Materials Science and Engineering, Saveh Branch, Islamic Azad University, Saveh, Iran.

[2] School of Materials Science and Engineering, Iran University of Science and Technology, Tehran, Iran.

[3] Center of Excellence for Advanced Materials, Iran University of Science and Technology, Tehran, Iran.

Abstract: *Mono dispersed nano SiC particles with spherical morphology were synthesized in this project by hydrolysis and condensation mechanism during sol gel processing. pH, temperature and precursor's ratio considered as the main parameters which could influence particles size. According to DLS test results, the smallest size of particles in the sol (<5nm) was obtained at pH<4. It can be observed from rheology test results optimum temperature for achieving nanometeric gel is about 60 ˚C. The optimum pH values for sol stabilization was (2-5) determined by zeta potentiometery. Si^{29} NMR analysis was used in order to get more details on final structure of gel powders resulted from initial sol. X-ray diffraction studies showed sythesized powder consists of β-SiC phase. Scanning electron microscopy indicated agglomerates size in β-SiC synthesis is less than 100 nm. Finally, TEM studies revealed morphology of β-SiC particles treated in 1500˚C and after 1hr aging is spherical with (20-30) nm size.*

Keywords: *carbides; nanostructures; sol-gel chemistry; nuclear magnetic resonance (NMR); microstructure.*

1. INTRODUCTION

Nowadays, advanced carbide ceramics are interesting materials for advanced ceramics and industrial applications due to their unique characteristics. Silicon carbide is known as an important non-oxide ceramic with high melting point (2827 °C), high hardness, high wear resistance, low thermal expansion coefficient, good chemical resistance and good thermal conduction in ceramic industry [1-3]. It is used in electrical and ceramic industries, high temperature engineering ceramic devices and as reinforcement for ceramic composites [4-7]. Different methods used for SiC particles synthesis are concluded of Acheson process, Si metals direct carburization, chemical vapor deposition (CVD), carbothermal reduction of silicon dioxide and sol gel technique. Some of these methods have disadvantages; for example, CVD process is a high cost and low efficiency method and Si metals direct carbonization will leave high amount of impurities in final powder. Therefore, using an appropriate method is required for SiC particles synthesis. Sol gel based methods which were reported in 1996 for the first time, have been widely reviewed by different authors [8]. This method has been established as a novel process for nano particles synthesis with several outstanding features, such as high purity [9], high chemical activity, improvement of powder sinter ability and possibility for particles mixing at molecular scale etc. Sol gel process using metal alkoxides has been widely applied for synthesis of ideal powders; homogeneous, size and shape controlled, and high purity [10]. Aelion et al. were among the first to investigate kinetics of hydrolysis and condensation of TEOS. The rate and extent of the hydrolysis reaction were found to be influenced by strength and concentration of acid or base catalyst while temperature and solvent were of secondary importance [11]. Colloidal aggregation and gelation play important roles in applications, including the colloidal processing of ceramics, solid–liquid separations and polymer dispersion processing [12]. Cheng et al studied the application of these carbosilane and polycarbosilane precursors in the preparation of SiC nanostructures by using a template [13]. Blute et al used several surface chemical techniques, which included dynamic light scattering, zeta potential, and kinematic viscosity to characterize a series of industrially manufactured colloidal silica particles within the 5–40 nm size range [14]. Jin et al proposed a

modified sol gel route for preparation of high surface area mesoporous SiC. The mesoporous SiC was obtained by heating a binary carbonaceous silicon xerogel under high temperatures [15].

The goal of this research is the study of the effective parameters on particles size in sol as pH and temperature to obtain SiC nano particles finer than 50 nm with semi-spherical morphology and homogenous particle size distribution.

2. MATERIAL AND METHODS

2. 1. Material

The chemicals used in this work were tetraethyl orthosilicate (TEOS, Merck Ag Germany Art No. 8006581000), choloridric acid (HCl, Merck Ag Germany Art No. 1003172500), Sodium Hydroxide (NaOH, Merck Ag Germany Art No. 1091372500), ethanol (Merck Ag Germany Art No. 100967), distilled water, phenolic resin (resol, RIL 800 Resitan Co., Iran) and acetone (Merck Ag Germany Art No. 1000142500) as resol solvent.

2. 2. Methods

At first, 60ml TEOS, 40ml water and 30ml ethanol were mixed and then solution of 50 g phenolic resin in 100 ml acetone was added. The solution under a reflux condition was homogenized by a magnetic stirrer. The pH of solution was controlled by introducing the sufficient amounts of catalyst (HCl, NaOH). At the next stage, hydrolysis reactions were completed and $Si(OH)_4$ particles were formed. Due to decreasing of alcohol amount, the solution was distilled by water to prevent rapid gel formation. In this stage the solution consisted of fine homogenized particles of Si $(OH)_4$ and phenolic resin that were fully soluble in it. By temperature increase, due to condensation reaction (water and alcohol condensation) the particles connected to each other and form polymers with siloxane (Si-O-Si) bonds. At this stage, chain-shaped structures which made by these new connections trapped the liquid phase into their interspaces. Also, carboneous phase was fully dispersed in the polymer structure at molecular level. The obtained wet gel was aged at room temperature and 1atm pressure for 24 hr in the oven. The molecular water of gel was evaporated at 110 ˚C and 1atm pressure and the obtained dried gel was named xerogel. In order to remove the structural water and organic matters, the gel powder was pyrolized at 700 ˚C for 1hr and heat treated at 1500°C for 1hr with 10 ˚C/min heating rate in an electrical furnace (carbolite 1600) at Ar atmosphere. Characterization methods included particle size measurements by Dynamic Light Scattering (DLS) using Malvern DTS system were used. In this method, the solubility rate is measured based upon the illumination of laser ray with less than 100nm wavelength in the sol. The suspended particles in the sol are constantly moving due to Brownian motions and in these movements they have some contacts with other particles beside them. The relationship between particles size and their Brownian motions speed is calculated from the Stokes-Einstein (equation (1, 2)) [16].

$$D=(k_B\ T)/6\pi\eta r \qquad (1)$$

$$\mu_p=1/6\pi\eta r \qquad (2)$$

Where D is the Diffusion coefficient, μp is the particles mobility, T is the solution temperature, η is solution viscosity and r is particles radius. Rheological measurements by Physica MCR300 instrument, sol stabilization by zeta potentiometery using Malvern DTS Zeta sizer, FT-IR studies by Shimadzu 8400S instrument, NMR results by the ^{29}Si MAS spectra were obtained that 11.7 T using a Varian Unity 500 spectrometer with a 7 ms 90° pulse and a delay time of 60s, phase analysis by XRD Philips Xpert system, scanning electron microscopy by SEM LEO 1455 vp and transmission electron microscopy by TEM Philips CM200 were done.

3. RESULTS AND DISCUSSION

3. 1. Effect of pH on Si (OH) 4 Particles Solution Rate

Figure 1 shows variations of solution rate vs.

pH, moreover in support of this figure, reaction (3) shows Alkoxide group hydrolysis. In this stage, OR groups are substituted by OH-functional groups. According to figure 1, at pH lower than 4, the solution rate was very low because of the low OH-concentration in the solution, so, the solution rate decreased as hydrolysis time increased. At pH range 4-7, by increasing OH- ion concentration, the rate of hydrolysis reaction and $Si(OH)_4$ particles formation increase. Finally at pH more than 7, the concentration of OH^- ions was higher than a critical value. So the solution rate increased significantly and its variations become more positive during the process.

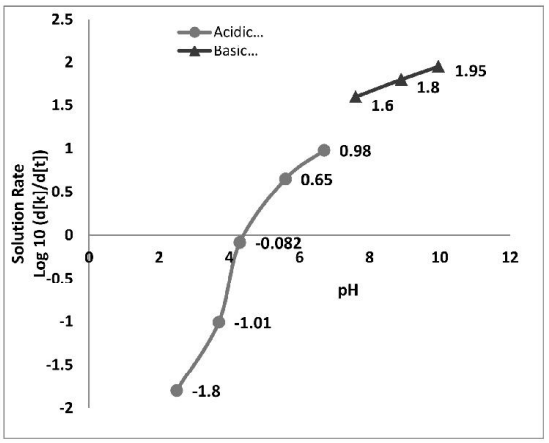

Fig. 1. Variations of solution rate vs. pH in the sol

$$Si(OR)+H_2O \xrightarrow{K_h} SiOH+ROH \qquad (3)$$

3. 2. Effect of pH on Si $(OH)_4$ Particles Size

Figure 2-I shows the particles size variations vs. pH and 2-II shows particles size distribution at pH 2.5-4. As it can be seen in figure 2-I, at acidic pH the particles size is less than that of basic condition. At lower pH ranges (<4) the size of particles was very fine and their variations were negligible even after aging because as OH-concentration was low, particles growth stopped when their sizes reached to 10 nm. As pH raised, the particles size was increased and its variations at before and after aging time increased, so simultaneous nucleation and growth of particles was occurred.

Figure 2-II shows particle size distribution in

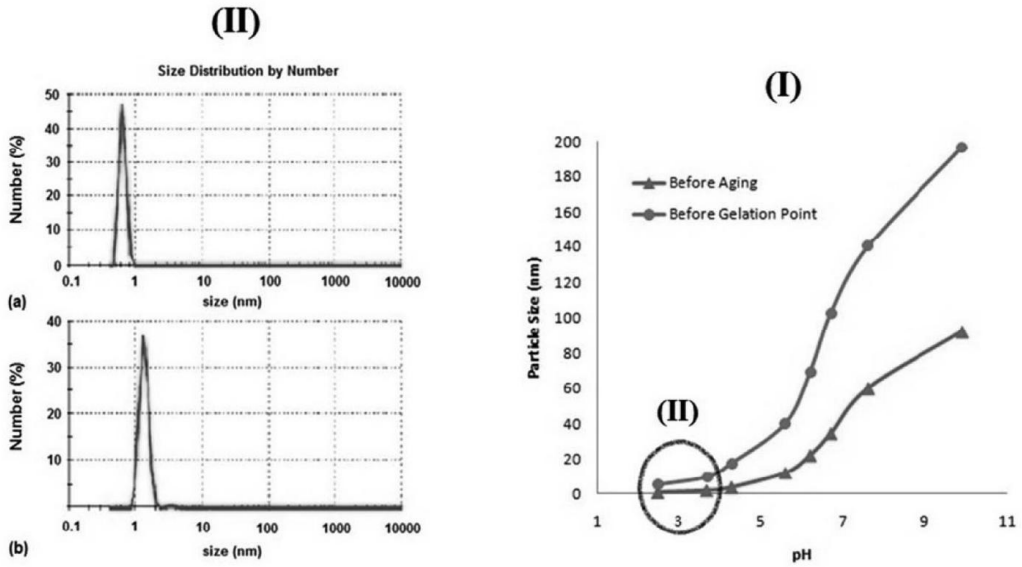

Fig. 2. (I) Variations of particles size vs. pH value range and (II) particles size distribution at pH 2.5 (a) before aging (b) before gelation time

the sol at pH value range 2.5-4. As it is illustrated, the particle size distribution which is observed at pH range 2.5-4, occurred in a narrow range and was monosized. A simultaneous and homogeneous particle generation occurred in the sol and negligible variation was observed between particles size before and after aging [17].

3. 3. Effect of pH on Gelation Time

Figure 3 shows gelation time variations vs. pH value. It can be seen that in acidic conditions and at pH range less than 4, gelation time was in its maximum amount because the precursor solubility was low in the sol. At the pH range 4-7, precursor's solubility was increased and gelation time reached to its minimum. Moreover, in this pH range primary groups with low molecular weights would convert to condensed groups by nucleation and growth mechanism.

At pH value more than 7 the polymerizations time increased to more than that of the acidic pH. Reaction (4) shows the excess OH- ions hydrolyzed and decomposed the siloxane bond (Si-O-Si) and inhibited the particles agglomeration due to the electrostatic repulsion. So all condensed polymers are ionic and are repulsive from both sides.

$$Si - O - Si + OH^- \rightarrow Si - O^- + Si - OH \qquad (4)$$

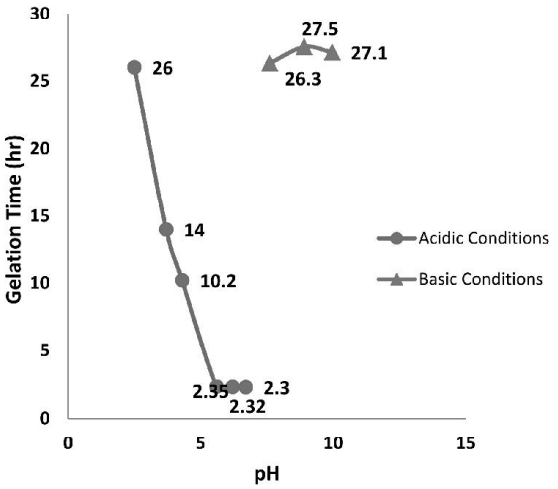

Fig. 3. The gelation time variations vs. pH value

3. 4. Effect of Precursor's Ratio on Gelation (Polymerization) Time

According to Fig. 4, the gelation time was minimized at H_2O/Si ratio of 7-9. At pH values lower than 7 the concentration of OH- is very low and at values greater than 9 the concentration exceeded to a critical value. Concentration of surface charges resulted in the ionization of condensed phases and due to this, the repulsion of silica particles was increased.

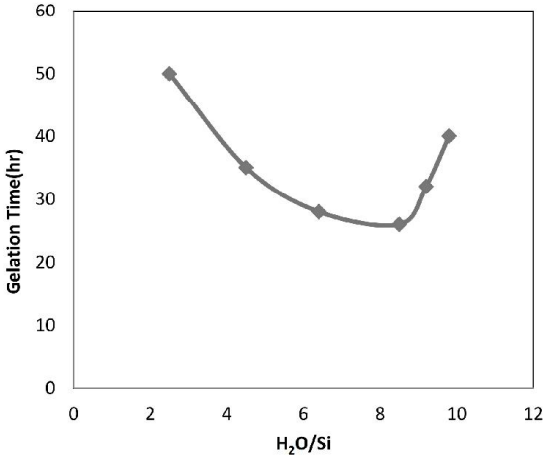

Fig. 4. Effects of H_2O/Si variation on gelation time

3. 5. Sol Stabilization Studies

Table 1 shows Zeta potential variation vs. pH value range. This table shows that at pH values lower than 4 the ideal zeta potential achieved for a stable colloidal system. At pH values between 6 and 7, the zeta potential tends to zero and minimum stability was achieved. In this condition the particles agglomeration occurred. At pH values more than 7, the absolute value of zeta potential increased and formed stable colloidal system.

This phenomenon could be explained by DLVO theory [10] which determines correlations between electrostatic repulsion and Van der Waals attraction forces. Initial particles which nucleate in the sol could be dispersed by a strong repulsion force. Equation (5) describes the relationship between surface potential and agglomeration:

$$V_B = -A\kappa a/12 + 2\pi\varepsilon a\psi^2 \qquad (5)$$

Table1. Zeta potential variation vs. pH value

pH	Zeta potential(mV)
2.5	32
3.7	31.8
4.5	16.4
5.6	8.6
6.2	1.4
6.9	-3.2
7.6	-18.4
8.9	-29.2
9.96	-38.3

Where V_B is energy barrier for prevention of agglomeration between two particles, A is Hamaker's constant, κ is Deby-Huckel factor, a is particle diameter, ϵ is dielectric constant of intermediate liquid and Ψ is surface potential. In this equation, first term which is negative is representative of Van der Waals attraction force contribution and second term which is positive is representative of electrostatic repulsion force contribution. So according to equation (5) in the pH range of 4-7 in which zeta potential and double layer thickness are in their minimum, V_B is very low and consequently the sol is unstable. In the pH range of 2.5-4, by zeta potential increasing, V_B increases. Thus it can be concluded that in the latter pH range, sol stability is in its maximum and particles size could be more controllable. Also in high pH range (7-10), absolute value of Zeta potential is high and led to a stable sol system.

3. 6. Effect of Temperature on Gelation Time and Mean Particles Size

Effects of temperature on gelation time and mean particle size were shown in figure 5. According to this figure, the rate of solution reaction was increased by increasing the temperature. So the probability of particles growth and the formation of condensed particles increased at high temperatures.

On the other hands, formed nucleus adhere together in the Sol and make the rings including the Si-O, Si-OR and Si-OH bonds that OH bands are on the surface of this rings (figure (6)) [18]. Higher Gel forming temperature leads to the higher ring adherence speed. Above results is confirmed by the Ostwald growth mechanism [18]. In this mechanism the light weight molecules dissolved and precipitated on the surface of the heavy weight molecules and lead to increasing of the particle size.

On the basis of mass fractal theory (equations (6), (7)) [19], the cluster volume and also the random rings volume increase with increasing the gel formation temperature. On the other hands, the gel density decreases at higher gel formation temperatures.

$$m \alpha r^{dm} \quad (6)$$

$$\rho \alpha (m/ r^{dm}) \quad (7)$$

Where, m is mass, r is particles radius, ρ is density and dm is called mass fractal dimension of the object. Whereas for a fractal $d_m<3$. It can be concluded that the particles size and the other properties of the sol can be controlled by the processing temperature and finally optimize the properties of the gel such as density etc. The exponential decay for gelation time vs. temperature elevation in this figure is confirmed by equation 8. According to this equation, the gelation time decrease at higher temperatures could be attributed to lower energy required for particles growth:

$$\frac{1}{t} = \exp\left(-\frac{Q}{RT}\right) \quad (8)$$

Where, T is temperature (°C), t is gelation time

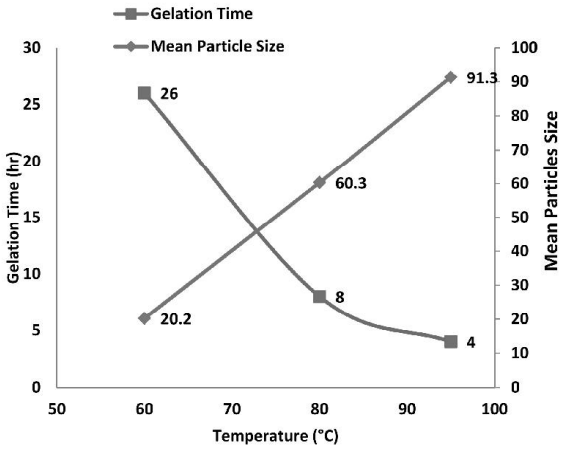

Fig. 5. Effects of temperature on gelation time and mean size of $Si(OH)_4$ particles.

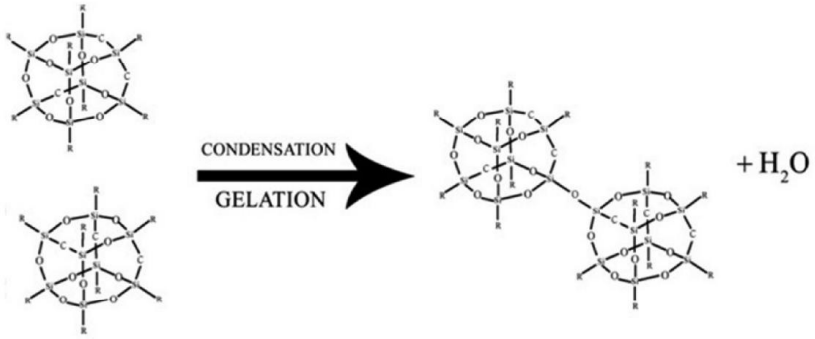

Fig.6. Adhesion bonding of the rings due to gelation process

(h) and Q is activation energy for particles growth.

3. 7. Powder Properties

Si^{29} MAS NMR analysis was performed on experimental sample which is shown in figure 7. Resonance peaks of gel powder containing carbon and silicon phases were examined during these analyses. These peaks were in the form of Q^n (n=2, 3, 4) in which n is the number of Si-O-Si bonds. In other word, Q^n is microstructure of silicon atom in $Si(OSi)_n$ $(OR)_{4-n}$ units which is $Q^2[Si(OSi)_2(OR)_2]$, Q^3 $[Si(OSi)_3(OR)]$ and Q^4 $[Si(OSi)_4]$. R is related to hydroxyl groups (OH-) or methylene groups ($-C_2H_5$). Si^{29} MAS NMR will give a wide range signals between -75 and -125 ppm which are corresponded to three different part with chemical transmission amounts of about -90 to -98 ppm, -98 to -105 ppm and -105 to -115 ppm related to Q^2, Q^3 and Q^4 regions. Figure 9 shows Si^{29} MAS NMR spectrum for synthesized gel powder in presence or absence of carbon phase. As it can be seen, the present signal of Q^4 in figure 7-a is in the range of -111.1 ppm which exhibits a high resonance

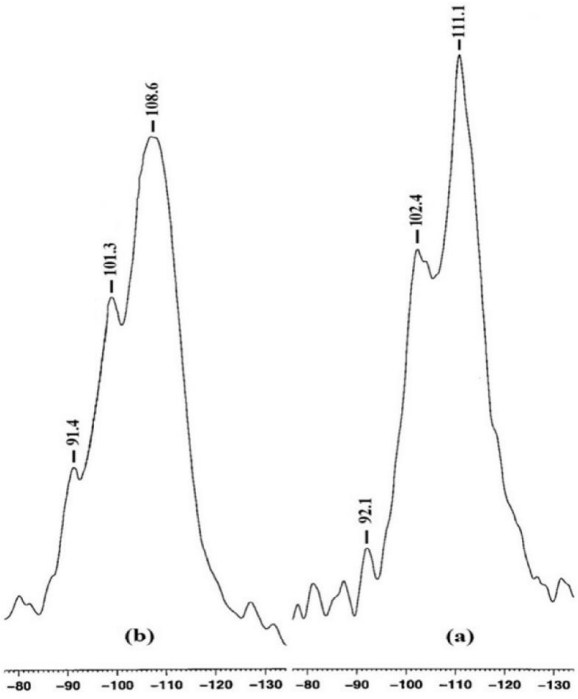

Fig. 7. ^{29}Si MAS-NMR spectra of the gel powder (a) without carbon phase and (b) with carbon phase

intensity. This signifies large number of silicon bonds which are formed during gelation process.

In frequency ranges of -102.4 ppm and -92.3 ppm, Q^3 and Q^2 silicons are observed, respectively, which indicates that during condensation stage OH^- and methylene ($-C_2H_5$) bonds are still presented on the surface of siloxane bonds. Figure 7-b shows NMR spectrum resulted from TEOS xerogel containing carbon phase. As it is observable, the signal presented at -111.1 ppm was shifted to -108.6 ppm due to the presence of Q^4 structural units which is related to formation of Si-O-C complex bonds and their effects on $Si(OSi)_4$ chemical transmissions; this finding could also be confirmed by FTIR spectrum(see figure (8)). On the other hand, the decrease in peaks intensity of Q^2 and Q^3 structural units is also observable within the spectrum resulted from the sample containing carbon phase. So, it can be concluded that presence of carbon phase in sample could change xerogel structures containing $Si(OSi)_4$ during sol-gel process and, moreover, it can also be concluded that carbon phase is leaked into the $Si(OSi)_4$ structure at molecular level.

Figure 8 shows the X-ray diffraction patterns of synthesized powder at pH 2.5 and H_2O/Si ratio of 8.5 and heated at 1500 ˚C for 1h It can be seen that main peaks of synthesized powder at

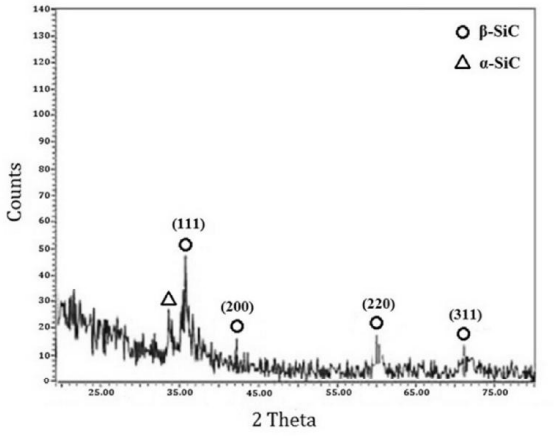

Fig. 8. X-ray diffraction pattern of synthesized SiC nano powder at 1500˚C

diffraction angles of (2θ) 35.6°, 41.3°, 60.1° and 72.1° are corresponded to {111}, {200}, {220} and {311} planes which are ascribed to cubic β-SiC phase. It should be noted that close to {111} planes peak between 2θ= 33° and 2θ=35° there is a shoulder which is related to SiC hexagonal polytypes which are usually appeared as α-SiC (2H, 4H, 6H etc). Finally, no peak is found to be related to Crystoballite phase and no silica phase could be detected at the sensitivity of X-ray diffraction [17]. The phase evaluation compares well with investigation carried out by C. Vix-

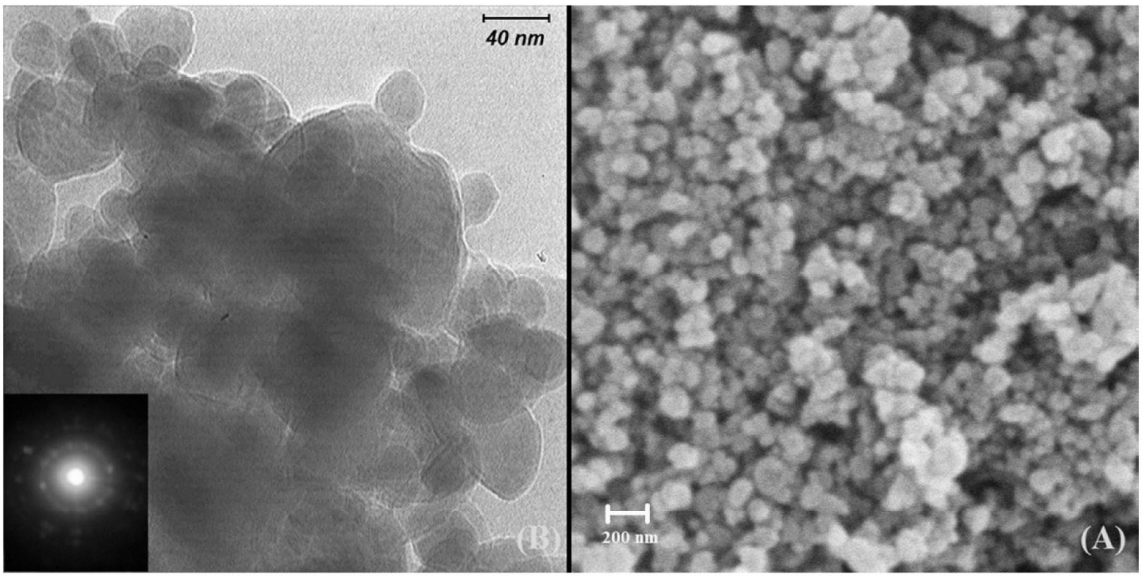

Fig. 9. (A) SEM and (B) TEM micrograph of synthesized nano powder at 1500˚C for 1h.

Guterl et al [20] .

Figure 9-A and 9-B shows the SEM and TEM micrographs of the synthesized powder with the previously mentioned characteristics, respectively. As it can be seen in figure 9-A, the resulted powders are monosized and homogeneously distributed with semi-spherical morphology. The size of formed agglomerates is estimated less than 100 nm. Also as it is illustrated by figure 9-B, the mean size of the particles is between 30-50 nm. As the diffraction pattern shows, these particles are polycrystalline and are in nano-metric range. The particles were observed to grow as semi-spherical shape. This, we believe, is due to controlled processing parameters such as time and temperature which are maintained under equilibrium conditions. In fact we noticed, for example, the morphology of β-SiC particles changes to whisker type at long soaking time. Also at higher temperatures when CO or SiO gases evolve, the particles were found to grow in rod shape habit.

4. CONCLUSIONS

In this research it is concluded that the effective parameters such as pH, temperature and precursors ratio can control the particles size in the sol. The pH effect was studied in both acidic and basic conditions. It was resulted that in very low pH in the range of 2.5-4, finest particles size could be obtained because particles size could be precisely controlled; hence, monosized particles would be provided. By temperature elevation, gelation time was decreased and mean particle size increased, so temperature with lowest mean particle size was applied (60 °C) and then gelation time was minimized by precursor's ratio variations. As a result, the best condition for sol aging was achieved at pH lower than 4 and 60°C gelation temperature. β-SiC phase was characterized by X-ray diffractometry at different plains. According to the scanning electron micrographs the agglomerates size was measured less than 100 nm. The polycrystalline particles size was determined between 30-50 nm with semi-spherical morphology by transmission electron microscopy.

REFERENCES

1. Shi, L., Zhao, H., Yan, Y., Li, Z., Tang, Ch., "Synthesis and characterization of submicron silicon carbide powders with silicon and phenolic resin", Powder Technology 169 (2006) 71–76.
2. Raman, V., Bahl, O. P., Dhawan, U., "Synthesis of silicon carbide through the sol-gel process from different precursors", Journal of Materials Science 30 (1995) 2686-2693
3. Larpkiattaworn, S., Ngernchuklin, P., Khongwong, W., Pankurddee, N., Wada, S., "The Influence of Reaction Parameters on The Free Si and C Contents in the synthesis of nano-sized SiC", Ceramics International 32(2006) 899-904
4. Lin, Y. J., Chuang, Ch. M., "The Effects of Transition Metals on Carbothermal synthesis of β-SiC powder", Ceramics International 33 (2007) 779-784
5. Kurtenbach, D., Mitchell, B. S., Zhang, H., Ade, M., Muller, E., "Crystallization kinetics of amorphous silicon carbide derived from polymeric precursors", Thermochimica Acta 337 (1999) 155-161
6. Koc, R., Glatzmaier, G., Sibold, J., Journal of Material Science 36 (2001) 995– 999.
7. Sharma, R., Sridhara Rao, D. V., Vankar, V. D., "Growth of nanocrystalline β-silicon carbide and nanocrystalline silicon oxide nanoparticles by sol gel technique", Materials Letters 62 (2008) 3174–3177.
8. Konno, H., Kinomura, T., Habazaki, H., Aramata, M., "Synthesis of submicrometer-sized β-SiC particle from the precursors composed of exfoliated graphite and silicone", Carbon 42 (2004) 737-744
9. Kurumada, K. I., Nakabayashi, H., Murataki, T., Tanigaki, M., "Structure and formation process of silica microparticles and monolithic gels prepared by the sol-gel method", Colloids and Surfaces A: Physicochemical and Engineering Aspects 139 (1998) 163–170
10. Seog, I., Kim, C. H., "Synthesis of silicon carbide through the sol-gel process from different precursors", Journal of Material Science 28 (1993) 3277-3282.
11. Bogush, G. H., and Zukoski, C. F., "Studies of

the kinetics of the precipitation of uniform silica particles through the hydrolysis and condensation of silicon alkoxides", Journal of Colloid and Inlerface Science, 142 (1991) 1-18.
12. Schantz Zackrisson, A., Pedersen, J. S., Bergenholtz, J., "A small-angle X-ray scattering study of aggregation and gelation of colloidal silica", Colloids and Surfaces A: Physicochem. Eng. Aspects 315 (2008) 23–30.
13. Cheng, Q., M., Interrante, L. V., Lienhard, M., Shen, Q., Wu, Zh., "Methylene-bridged carbosilanes and polycarbosilanes as precursors to silicon carbide—from ceramic composites to SiC nanomaterials", Journal of the European Ceramic Society 25 (2005) 233–241.
14. Blute, I., Pugha, R. J., Van de Pas, J., Callaghan, I., "Industrial manufactured silica nanoparticle sols". 2: Surface tension, particle concentration, foam generation and stability, Colloids and Surfaces A: Physicochem. Eng. Aspects 337 (2009) 127–135.
15. Guo-Qiang, J., Xiang-Yun G., "Synthesis and characterization of mesoporous silicon carbide", Microporous and Mesoporous Materials 60 (2003) 207–212.
16. Einstein, A., "Investigations on the theory of the brownian movement", Annalen der Physik, 17 (1905) 549–560.
17. A., Najafi, Golestani-Fard, F., Rezaie, H. R., Ehsani, N., "Effect of APC addition on stability of nanosize precursors in sol–gel processing of SiC nanopowder", Journal of Alloys and Compounds, 505(2010) 692-697
18. Brinker, C. J., and Scherer, G. W., "The physic and chemistry of sol gel processing, Academic Press, 1990
19. Rahaman, M. N., "Ceramic Processing and Sintering", 2nd ed., Marcel Dekker, New York, 2003, chap.11
20. Vix-Guterl, C., Alix, I., Ehrburger, P., "Synthesis of tubular silicon carbide (SiC) from a carbon–silica material by using a reactive replica technique": mechanism of formation of SiC Acta Materialia 52 (2004) 1639–1651.